Infrared Spectroscopy Studies of Structure and Orientation in Clay-Reinforced Polyamide-6 Nanocomposites

Kenneth C. Cole, Johanne Denault, Martin N. Bureau*

National Research Council Canada, Industrial Materials Institute, 75 De Mortagne Blvd., Boucherville, Québec, Canada J4B 6Y4

Summary: Infrared (IR) spectroscopy was used to study the surface (by means of external reflection) and the bulk (by means of transmission measurements on microtomed slices) of specimens obtained by injection moulding of a commercial polyamide-6 clay-based nanocomposite material (NCH = nylon clay hybrid) at different mould temperatures and with different part geometries. Comparisons were made with equivalent non-reinforced polymer (PA-6). For the PA-6, the mould temperature influences the crystalline structure, with the γ phase predominating at 50°C and the α phase at 80°C. However, in the NCH material the γ phase is favoured, even at 80°C. In all cases the crystallinity increases on going from the surface to the core. The polymer chains are oriented in the flow direction, and the orientation is higher for parts with more elongated shapes. It does not vary greatly across the part thickness, except for a thin surface layer, where it is significantly higher. Both at the surface and in the bulk, the crystalline phase orientation is higher for the NCH than for the PA-6.

Keywords: infrared spectroscopy; nanocomposites; nylon; orientation; polyamides

Introduction

The benefits of using inorganic particles or fibres as reinforcing material in a polymeric matrix have been recognized for a long time, but it is only over the last twenty years or so that the particular advantages of polymer nanocomposites have become widely appreciated. These consist of materials in which at least one of the dimensions of the reinforcing particles is in the nanometre range. The most common type of reinforcement that is being exploited currently is based on naturally occurring silicates like montmorillonite clay.[1] The crystalline structure of such materials involves silicate layers that are only one nanometre thick and are relatively loosely bound to each other by cations like Na^{+} and Ca^{++} that counterbalance the net negative charge on the layer surface. If the clay is treated with a cationic organic intercalant like a quaternary ammonium compound, the latter penetrates between the layers, replaces the inorganic cations,

 DOI: 10.1002/masy.200450105

and increases the distance between the layers. Mixing with a molten polymer resin results in further intercalation and, ideally, full exfoliation, where the individual silicate layers are fully separated. Alternatively, the clay can be mixed with a liquid monomer that is subsequently polymerized in situ. Exfoliation leads to a large number of particles with high surface area, with the possibility for much more matrix-reinforcement interaction than occurs in conventional composites. As a result, a relatively low level of clay (less than 5 wt%) can produce significant improvements in various properties, including mechanical, barrier, heat deflection, and flame resistance. However, such gains are not always easily achieved. Considerable research is being devoted to the development of technologies to achieve full exfoliation and to optimize the clay-polymer interface, particularly when the polymer is hydrophobic and therefore incompatible with the hydrophilic clay surface. Other research focuses on how the clay affects the microstructure of the polymer matrix, and hence its ultimate performance.

One of the first nanocomposite materials to be commercialized was developed by Toyota Central Research and Development Labs, Inc.[2-4] They treated sodium montmorillonite first with an ω-amino acid as intercalant, then with ε-caprolactam monomer, then polymerized the monomer in situ to produce nylon 6-clay hybrid (NCH). Compared to neat polyamide-6, the presence of only 4.7 wt% clay in the NCH increased the heat deflection temperature from 65°C to 152°C, the room-temperature tensile modulus from 1.1 to 1.9 GPa, and the tensile strength from 69 to 97 MPa, while only slightly reducing the Izod impact strength from 21 to 18 $J \cdot m^{-1}$. In this work, injection-moulded specimens made from similar materials were studied by infrared (IR) spectroscopy with the aim of elucidating differences in microstructure that might contribute to the superior performance of the NCH. The infrared spectrum of polyamide-6 and its relationship to crystalline structure and orientation are described in a recent publication on polyamide-6 films.[5]

Experimental

The nanocomposite material used was NCH 1015C2 from Ube Industries, containing 2 wt% of layered silicate. It was compared with Ube's equivalent grade of unmodified polyamide-6, 1015B. Both materials were injection-moulded at a melt temperature of 255°C and at three different mould temperatures, namely 50°C, 65°C, and 80°C. The mechanical performance of these materials was reported previously.[6] Specimens with the three different geometries shown

in Figure 1 were analyzed by IR spectroscopy. Two sets of samples were analyzed – one involving the three geometries all injected at a mould temperature of 65°C, the other involving only dogbones but injected at the three different mould temperatures. For orientation measurements, the "machine" direction was defined as parallel to the direction of flow at the point of entry of the molten polymer, as shown in Figure 1.

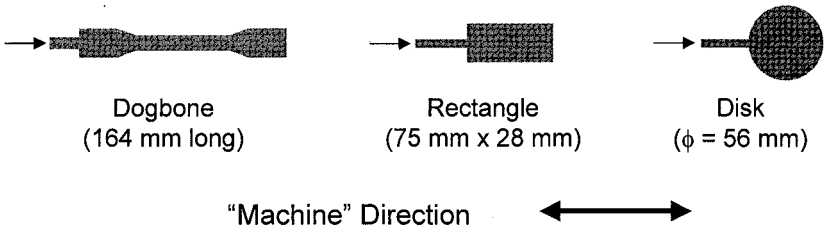

Fig. 1. Dimensions of injection moulded specimens. The thickness was 3.2 mm in all cases.

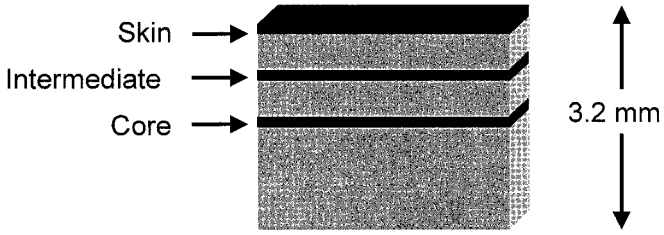

Fig. 2. Microtoming of dogbone specimens to obtain slices for transmission measurements.

IR spectroscopic measurements were made on a Thermo Nicolet Magna 860 Fourier transform instrument equipped with a DTGS detector; each spectrum corresponded to an accumulation of 128 scans at a resolution of 4 cm^{-1}. The surface of all the samples was analyzed at the specimen centre by external specular reflection, with the use of a HSR134 accessory from Spectra-Tech (angle of incidence 11°). For certain dogbone samples, the interior of the specimens was also analyzed. Slices about 30 μm thick were cut with a microtome from the narrow portion of the dogbone as shown in Figure 2. They were taken at three different depths: skin (0 – 300 μm), intermediate (650 – 950 μm), and core (1450 – 1750 μm). The slices were analyzed in transmission with the use of a 4X beam condenser from Harrick Scientific Corp. to reduce the

beam size. A Spectra-Tech zinc selenide wire grid polarizer was used to control the beam polarization. Special treatments of the spectral data like Kramers-Kronig transformation and curve fitting were done with GRAMS/32 software from Galactic Industries.

Differential scanning calorimetry was performed from 30°C to 250°C at a rate of 20°C per minute on a Perkin Elmer DSC-7 instrument.

Results and Discussion

Front-surface external reflection has been shown to be a useful technique for studying the surface of oriented polymer samples.[7] Although the spectra as measured are "distorted" by contributions from the refractive index, the Kramers-Kronig transformation makes it possible to separate the contributions of the refractive index and the absorption index. From these one can calculate the imaginary part of the complex molecular polarizability, which is considered to be the quantity most closely related to molecular properties in terms of band shapes and intensities.[7,8] Figure 3 shows typical spectra, corresponding to one of the samples analyzed here (polyamide-6 dogbone, mould temperature 50°C). The other samples showed qualitatively similar behaviour. The difference between the spectra measured with polarization parallel and perpendicular to the machine direction clearly shows the presence of orientation. If the orientation is assumed to be uniaxial, the structural factor spectrum can be calculated as SF = (Par + 2*Perp)/3. The SF spectrum is independent of orientation effects and can give information on other aspects, like crystalline structure and molecular conformation. The difference spectrum "Par – Perp", on the other hand, shows up the orientation more clearly, because only the bands that show dichroism will appear. Thus, in Figure 3, negative absorption is seen for the following bands: N–H stretching (3302 cm^{-1}), C–H stretching (2933 and 2859 cm^{-1}), Amide I (1643 cm^{-1}), CH_2 deformation in the α crystalline phase (1463 and 1418 cm^{-1}), and CH_2 twisting-wagging at 1172 cm^{-1}. These are all bands that have a transition moment more-or-less perpendicular to the polymer chain axis.[5] Bands that have a transition moment parallel to the chain axis, on the other hand, appear as positive in the difference spectrum. These include the Amide II band at 1548 cm^{-1}, as well as the skeletal modes at 1368, 1264, 1236, 1202, and 1123 cm^{-1}.

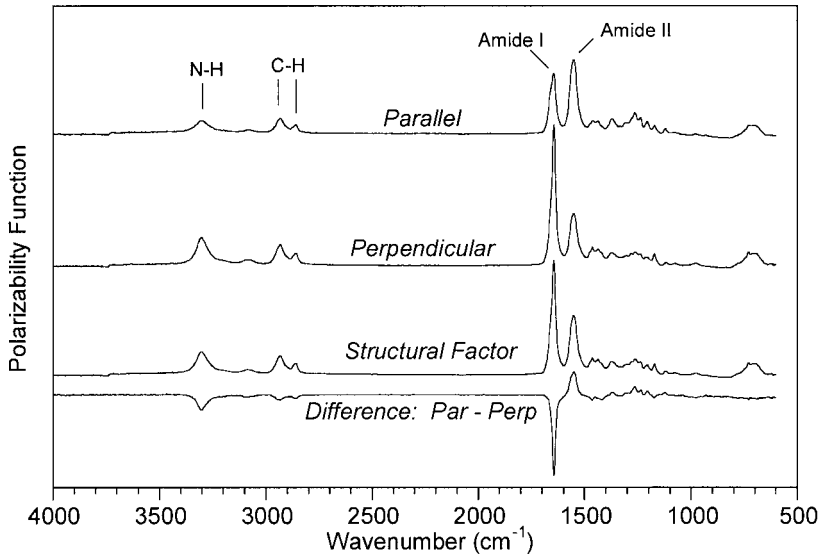

Fig. 3. Typical spectra obtained by front-surface external reflection (polyamide-6 dogbone, mould temperature 50°C).

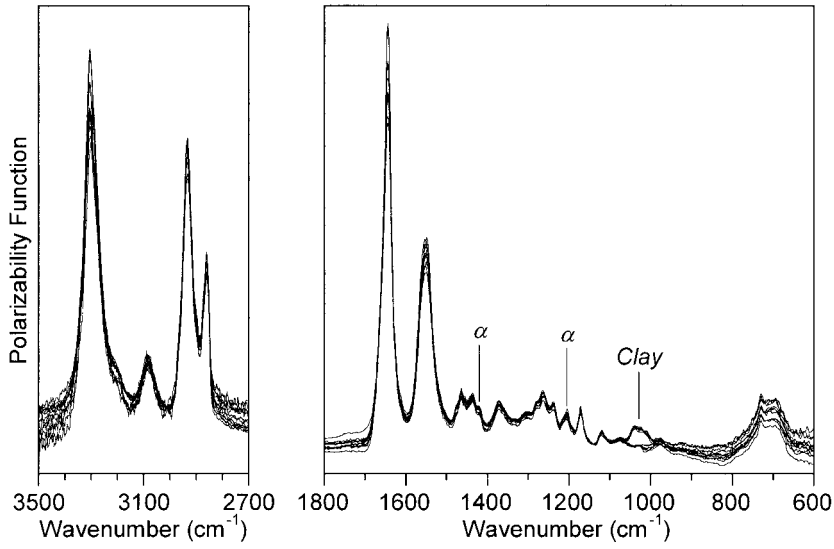

Fig. 4. Superimposed structural factor spectra for twelve injection-moulded samples.

Figure 4 compares the SF spectra obtained for the twelve different samples analyzed. Little variation is observed, the only obvious difference being that the clay peak at 1060-1000 cm^{-1} is present in the NCH spectra but not in the PA-6 spectra. All the samples show a similar and rather low level of crystallinity at the surface, as can be seen from the relative weakness of the α phase peaks at 1418 and 1202 cm^{-1}. This is to be expected from the rapid quenching of the molten polymer on contact with the cooler mould surface.

Because the Amide I and Amide II bands show the strongest dichroism (Figure 3), they were selected for quantitative characterization of the orientation. For the case of uniaxial orientation, the Hermans orientation function f is related to the dichroism of a particular vibrational band through the equation:

$$f = \frac{D-1}{D+2} \times \frac{2}{3\cos^2\alpha - 1}$$

where α is the angle between the polymer chain axis and the transition moment of the vibrational mode responsible for the band, and the dichroic ratio D is equal to the ratio of the band intensities in the spectra measured with polarization parallel and perpendicular to the machine direction. In this work, the dichroic ratios were determined by interactively subtracting the "Perp" spectrum from the "Par" spectrum and adjusting the subtraction factor until the band disappears. However, in the case of the Amide I band this is complicated by the fact that, as shown by Skrovanek, Painter, and Coleman for polyamide-11, this band involves three different components arising from three types of amide groups: non-hydrogen-bonded, "disordered" hydrogen-bonded, and "ordered" hydrogen-bonded.[9] At room temperature, the contribution from non-hydrogen-bonded species is very weak. Curve fitting of the SF spectra obtained here gave results very similar to those of Skrovanek et al., namely a good fit with two bands: the broad "disordered" band centred at 1648 cm^{-1} with a width at half height of 35 cm^{-1}, and the narrow "ordered" band at 1643 cm^{-1} with a width of 14 cm^{-1}. The implications for determining dichroic ratios are illustrated in Figure 5. In both the "Par" and "Perp" spectra, the Amide I band is clearly asymmetric and involves more than one component. When the two are subtracted with a factor of 0.210, as in spectrum Sub1, the narrow Amide I peak is cancelled out, leaving the symmetrical broad peak at 1648 cm^{-1}. When the subtraction factor is equal to 0.971 (spectrum Sub2), the broad Amide I peak is cancelled and a (negative) symmetric narrow peak remains at 1643 cm^{-1}.

Finally, when the subtraction factor is equal to 1.531 (spectrum Sub3), the Amide II peak disappears. There was no evidence that the Amide II band involves two components like the Amide I band. Again, this is in agreement with the observations of Coleman, Skrovanek, and Painter.[10]

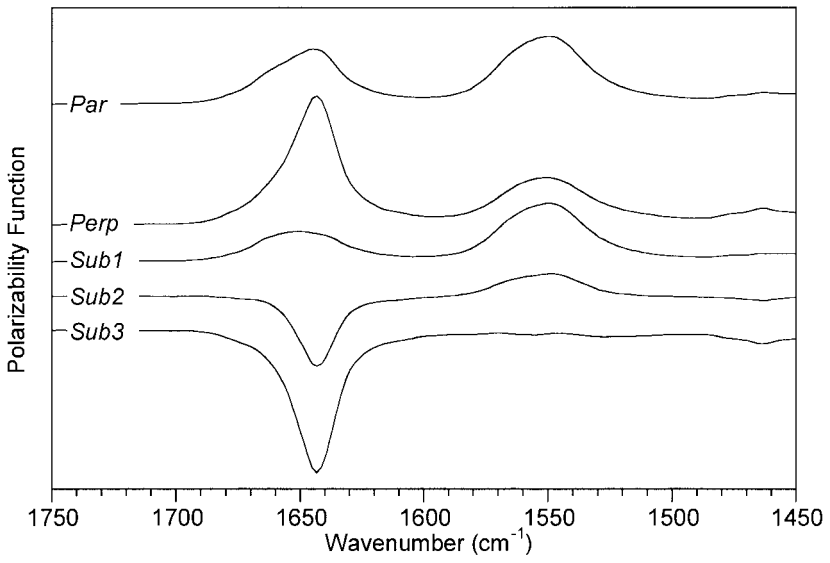

Fig. 5. Determination of dichroic ratios by subtraction for polyamide-6 dogbone, mould temperature 50°C: Sub1 = Par – 0.210 Perp; Sub2 = Par – 0.971 Perp; Sub3 = Par – 1.531 Perp.

Because the angles of the transition moments are not precisely known for the Amide I and Amide II bands, the orientation function f could not be calculated. Instead the "orientation parameter" (D-1)/(D+2) was calculated and is shown for the different samples in Table 1. This quantity is proportional to f and its magnitude is an indicator of the orientation, although it is positive for parallel bands and negative for perpendicular bands.

Table 1. Orientation parameters (D-1)/(D+2) calculated for the Amide I and Amide II bands in the surface reflection spectra of the different samples (PA-6 = neat polyamide 1015B, NCH = nylon clay hybrid 1015C2).

Geometry – Mould Temp.	Amide I (disordered)		Amide I (ordered)		Amide II	
	PA-6	NCH	PA-6	NCH	PA-6	NCH
Disk – 65°C	–0.014	+0.001	–0.230	–0.235	+0.078	+0.089
Rectangle – 65°C	–0.025	–0.048	–0.282	–0.300	+0.100	+0.133
Dogbone – 65°C	–0.046	–0.055	–0.342	–0.387	+0.166	+0.202
Dogbone – 50°C	–0.010	–0.006	–0.358	–0.387	+0.150	+0.206
Dogbone – 65°C	–0.042	–0.043	–0.344	–0.361	+0.148	+0.174
Dogbone – 80°C	–0.073	–0.072	–0.361	–0.405	+0.157	+0.196

Comparison of the results for the dogbones moulded at 65°C in each of the two sets shows generally good agreement and gives an indication of the experimental error involved. The results are precise enough that certain trends can be clearly discerned. First of all, as expected, the orientation is related to the specimen geometry and in all cases increases in the order disk < rectangle < dogbone. Secondly, the crystalline phase (which contributes to the "ordered" Amide I band and the Amide II band) and the amorphous phase (which gives rise to the "disordered" Amide I band) appear to show different behaviour. In the case of the crystalline material, the nanocomposite NCH shows higher orientation than the neat PA-6; this effect is very clear for the Amide II band, but somewhat less pronounced for the "ordered" Amide I band. Furthermore, the mould temperature has no obvious effect. For the amorphous material, on the other hand, there is no obvious difference between PA-6 and NCH, but the orientation appears to increase somewhat with the mould temperature.

It is well known that in injection-moulded parts made from a semicrystalline polymer the surface can be quite different from the interior, and for thick parts it is of course the interior that mainly determines the mechanical performance. To examine the interior structure, three dogbones were selected for more detailed analysis by microtoming and transmission measurements: PA-6 moulded at 50°C, PA-6 moulded at 80°C, and NCH moulded at 80°C. As was done for the surface reflection spectra, the spectra measured with polarization parallel and perpendicular to the

machine direction were used to calculate structural factor and difference spectra. A typical result is shown in Figure 6; the others were qualitatively similar. Because of the samples' thickness, the main bands are totally absorbing in the transmission spectra, so only the 1500 – 500 cm^{-1} region can be analyzed. For comparison, the difference spectrum "Par – Perp" from the surface measurement on a similar sample is also included, and it is reassuring to see that the dichroism observed at the core is similar to that seen at the surface. While most of the peaks showing dichroism arise from the α crystalline phase, dichroism can also be clearly seen for two "non-α" peaks at 1171 and 975 cm^{-1}.

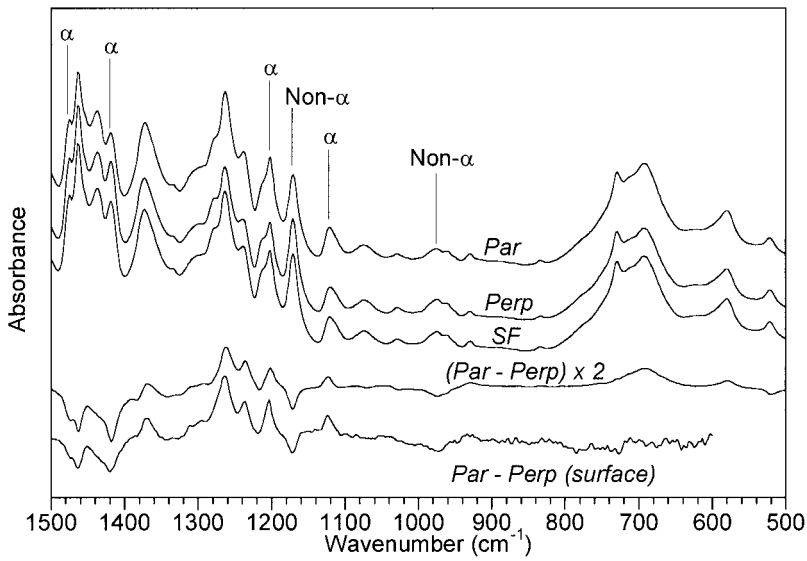

Fig. 6. Typical spectra obtained from transmission measurement on microtomed slice (polyamide-6 dogbone, mould temperature 80°C, slice from core). The "Par – Perp" spectrum from the reflection measurement at the surface is included for comparison.

Figure 7 compares the SF spectra for the three different dogbone samples at three different depths. In contrast with the surface spectra of Figure 4, significant variations are apparent. The PA-6 sample moulded at 80°C (curves d, e, and f) shows a considerably higher content of the α crystalline phase than do the other samples. This can be seen from the prominence of the peaks at 1418 cm^{-1}, 1202 cm^{-1} (compared to its neighbours at 1232 and 1171 cm^{-1}), 960 cm^{-1}, 930 cm^{-1},

692 cm^{-1} (Amide V), and 580 cm^{-1} (Amide VI). This sample also contains a significant amount of the mesomorphic β phase, which gives rise to the peak at 975 cm^{-1}. It is also noteworthy that the content of α phase increases in the order d < e < f, i.e. on going from the skin to the core. This is in keeping with the low α content observed in the surface spectra (Figure 4), and is consistent with the slower cooling expected for the core. Compared to the PA-6 sample moulded at 80°C, both the PA-6 sample moulded at 50°C and the NCH sample moulded at 80°C show lower content of the α phase and higher content of the γ phase. Although the β and γ phases give very similar infrared spectra, they can be distinguished by the fact that the γ phase gives a sharper peak at 975 cm^{-1} as well as a weak but distinct peak at 1000 cm^{-1}. The latter peak can be detected (barely) in the spectra of the PA-6 50°C sample (curves a, b, c), but in those of the NCH 80°C sample (curves g, h, i) it is masked by the broad clay peak at 1060-1000 cm^{-1}. Although it is difficult to see in Figure 7, spectral subtraction indicates that for both of these samples, the intermediate and core slices have a higher content of γ phase than does the skin slice. The infrared spectroscopy results are supported by the DSC results shown in Figure 8, where the melting transition of the γ phase occurs near 214°C and that of the α phase near 223°C. It is well known that, although the α phase is the one that is thermodynamically favoured in polyamide-6, the inclusion of nanoclay favours the presence of the γ phase.[11-14] The reason is believed to be that tethering of amino end groups to the clay surface forces the polymer chains to adopt the parallel alignment found in the γ phase and hinders the anti-parallel (head-to-tail) alignment required for the α phase.

As for the surface reflection spectra, the orientation parameter (D-1)/(D+2) was calculated by means of interactive spectral subtraction. However, because of the saturation of the Amide I and Amide II bands, it was necessary to use different bands, namely those at 1418, 1124, and 1170 cm^{-1}. The band at 1418 cm^{-1} is associated exclusively with the α phase and corresponds to a CH_2 deformation mode; its transition moment angle should be close to 90°. The band at 1124 cm^{-1} is also associated with the α phase; its transition moment angle is unknown, but it is more parallel than perpendicular. This band overlaps with non-α-phase bands at 1121 and 1119 cm^{-1}, but the spectral subtraction approach makes it possible to determine the dichroic ratio for the 1124 cm^{-1} component. Finally, the 1170 cm^{-1} band is known to arise mainly from non-α phases; again, its transition moment angle is unknown, but it is more perpendicular than parallel.[5]

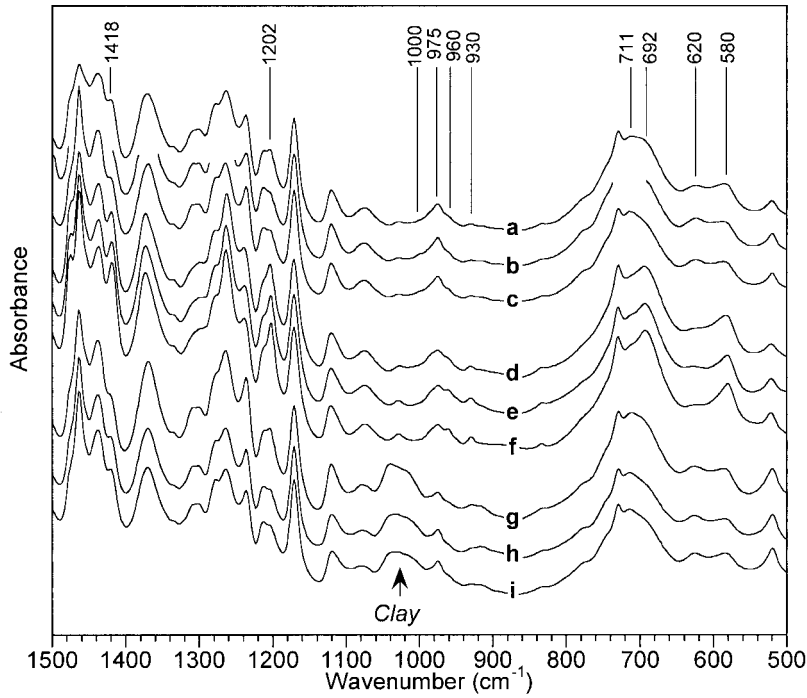

Fig. 7. Structural factor spectra for microtomed slices from: (a, b, c) PA-6, mould temperature 50°C, at skin, intermediate, and core levels respectively; (d, e, f) PA-6, mould temperature 80°C, at skin, intermediate, and core levels respectively; (g, h, i) NCH, mould temperature 80°C, at skin, intermediate, and core levels respectively. The gaps in curve b correspond to regions of saturation.

The calculated orientation parameters are given in Table 2. They are generally rather low compared to those determined for the surface spectra. For example, the 1418 cm^{-1} peak gives values in the range of –0.08 to –0.15. For the surface spectra of the dogbone samples, the "ordered" Amide I band, which also arises from the crystalline phase and is expected to have a similar transition moment angle near 90°, gives values in the range –0.34 to –0.41, or about three times higher. Thus the rapid quenching on contact with the mould surface produces a very thin surface layer with significantly higher orientation but relatively low crystallinity. The slower cooling at the core allows for relaxation of the molecular orientation and rearrangement into the crystalline structure.

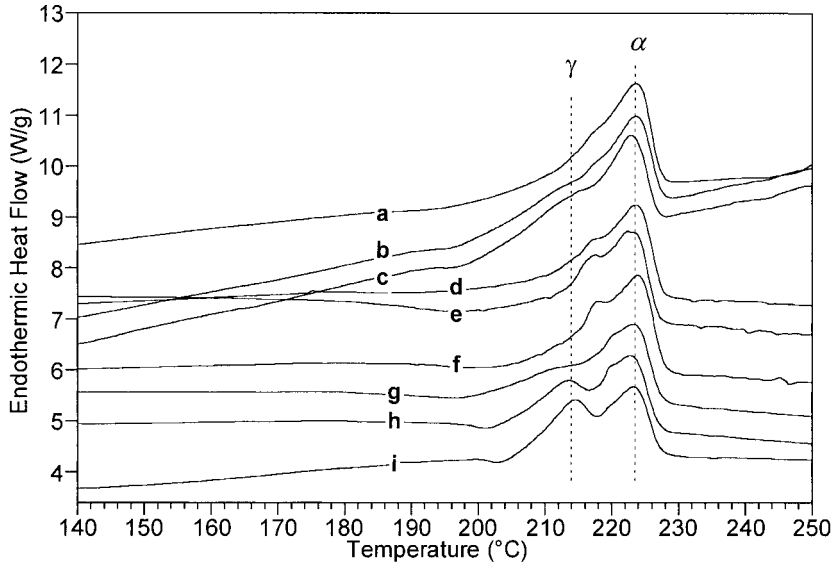

Fig. 8. DSC results obtained for microtomed slices similar to those analyzed by infrared spectroscopy: (a, b, c) PA-6, mould temperature 50°C, at skin, intermediate, and core levels respectively; (d, e, f) PA-6, mould temperature 80°C, at skin, intermediate, and core levels respectively; (g, h, i) NCH, mould temperature 80°C, at skin, intermediate, and core levels respectively.

Table 2. Orientation parameters (D-1)/(D+2) calculated for three bands in the transmission spectra of microtomed slices (PA-6 = neat polyamide 1015B, NCH = nylon clay hybrid 1015C2).

Mould temperature and slice position	1418 cm^{-1} (α phase)		1124 cm^{-1} (α phase)		1170 cm^{-1} (non-α phases)	
	PA-6	NCH	PA-6	NCH	PA-6	NCH
80°C – skin	–0.086	–0.105	+0.075	+0.034	–0.053	–0.031
80°C – intermediate	–0.113	–0.149	+0.095	+0.096	–0.058	–0.034
80°C – core	–0.076	–0.129	+0.093	+0.092	–0.045	–0.001
50°C – skin	–0.144		+0.067		–0.041	
50°C – intermediate	—		+0.051		–0.018	
50°C – core	–0.103		+0.069		–0.005	

Given the rather low level of orientation observed, it is difficult to discern any trends from the data in Table 2. There does not appear to be a significant effect of mould temperature or position within the sample (except for the very thin surface layer just discussed). However, for the α-phase band at 1418 cm^{-1} the NCH gives values of consistently higher magnitude than the PA-6. The same was observed for the surface spectra. For the α-phase band at 1124 cm^{-1}, on the other hand, there is no significant difference, and for the non-α-phase band at 1170 cm^{-1} the effect is reversed—the PA-6 values are of higher magnitude than the NCH ones. The situation is thus rather complicated, and further work is required before these results can be fully interpreted. The high shear fields present during injection moulding are expected to produce orientation of both the polymer chains and the clay sheets, but tethering of the chains to the clay surface could result in a complex interplay of opposing forces. Varlot et al. used small angle X-ray scattering to study the orientation of the clay sheets in polyamide-6 nanocomposites.[13] They found the nanocomposites to be highly anisotropic, with the montmorillonite sheets oriented around the injection axis and showing a preference to lie parallel to the large side of the rectangular part. Usuki et al. also observed, by means of transmission electron microscopy, strong alignment of the clay layers in polyamide-6 nanocomposites.[15] The nanocomposite spectra reported herein show a doublet clay peak at 1060-1000 cm^{-1} with maxima near 1044 and 1014 cm^{-1}, but this peak did not show any significant dichroism. However, if the platelets are aligned parallel to the surface one should not expect any difference between the spectra corresponding to the machine and transverse directions. To see the anisotropy it is necessary to obtain the spectrum corresponding to the normal or thickness direction. Provided the specimens are large enough, this could be done by means of the "tilted film" method as was done for biaxially oriented films.[5] Such films show not only preferential alignment of the polymer chains, but also of the hydrogen-bonded planes that are present in polyamide-6. This effect may also exist in the injection-moulded samples and could influence the results. For instance, bands that have their transition moment parallel to the polymer chain (like the Amide II band in Table 1) will be less sensitive to this effect and will therefore give a better indication of the chain orientation. The analysis thus becomes very complicated, especially when the different phases can show different orientation behaviour. The present work ignores these effects and is therefore only a first approximation, but further work is planned to explore these phenomena in greater detail.

Conclusions

The spectroscopic data obtained provide useful information on crystallinity and orientation in injection-moulded parts made from Ube NCH polyamide-6 nanocomposite, and on how they differ from those made from polyamide-6 alone (PA-6). In particular, it was confirmed that:

(a) In PA-6 the mould temperature influences the crystalline structure. A significant amount of γ phase is observed at 50°C but the more stable α phase is formed at 80°C.

(b) In the nanocomposite material NCH, the γ phase is strongly favoured over the α phase.

(c) In both cases, the crystallinity increases on going from the surface to the core.

(d) The molecular orientation at the centre of the part surface depends on the part geometry, being higher for more elongated parts. For the crystalline phase it is fairly high and independent of the mould temperature. For the amorphous phase it is much lower but increases somewhat with the mould temperature.

(e) The orientation does not vary much across the part thickness, except for a thin surface layer, where it is significantly higher.

(f) Both at the surface and in the bulk, the crystalline phase orientation is higher for NCH than for PA-6. However, there is no difference for the amorphous phase, at least at the surface; data could not be obtained for the bulk.

[1] M. Alexandre, P. Dubois, *Mater. Sci. Eng.*, **2000**, *28*, 1.
[2] A. Usuki, M. Kawasumi, Y. Kojima, A. Okada, T. Kurauchi, O. Kamigaito, *J. Mater. Res.*, **1993**, *8*, 1174.
[3] A. Usuki, Y. Kojima, M. Kawasumi, A. Okada, Y. Fukushima, T. Kurauchi, O. Kamigaito, *J. Mater. Res.*, **1993**, *8*, 1179.
[4] Y. Kojima, A. Usuki, M. Kawasumi, A. Okada, Y. Fukushima, T. Kurauchi, O. Kamigaito, *J. Mater. Res.*, **1993**, *8*, 1185.
[5] K. C. Cole, C. Depecker, M. Jutigny, J.-M. Lefebvre, P. Krawczak, *Polym. Eng. Sci.*, in press.
[6] M. N. Bureau, J. Denault, F. Glowacz, *Proc. SPE Ann. Tech. Conf. (ANTEC)*, **2001**, 2125.
[7] K. C. Cole, A. Ajji, E. Pellerin, *Macromolecules*, **2002**, *35*, 770.
[8] J. E. Bertie, S. L. Zhang, C. D. Keefe, *J. Mol. Struct.*, **1994**, *324*, 157.
[9] D. J. Skrovanek, P. C. Painter, M. M. Coleman, *Macromolecules*, **1986**, *19*, 699.
[10] M. M. Coleman, D. J. Skrovanek, P. C. Painter, *Makromol. Chem., Macromol. Symp.*, **1986**, *5*, 21.
[11] L. J. Mathias, R. D. Davis, W. L. Jarrett, *Macromolecules*, **1999**, *32*, 7958.
[12] D. M. Lincoln, R. A. Vaia, Z.-G. Wang, B. S. Hsiao, *Polymer*, **2001**, *42*, 1621.
[13] K. Varlot, E. Reynaud, M. H. Kloppfer, G. Vigier, J. Varlet, *J. Polym. Sci.: Part B: Polym. Phys.*, **2001**, *39*, 1360.
[14] M. N. Bureau, J. Denault, K. C. Cole, G. D. Enright, *Polym. Eng. Sci.*, **2002**, *42*, 1897.
[15] A. Usuki, N. Hasegawa, H. Kadoura, T. Okamoto, *Nano Letters*, **2001**, *1*, 2